Electrical characterisations and surface morphologies of thermally evaporated thin film silicon on plastic substrates for solar cells applications

M. Z. PAKHURUDDIN[*], K. IBRAHIM, A. ABDUL AZIZ
Nano-Optoelectronics Research and Technology Laboratory School of Physics, Universiti Sains Malaysia, 11800 Penang, Malaysia

Samples of thin film silicon (Si) on polyethylene terephthalate (PET) plastic with different Al doping levels (Al/Si ratio) were prepared by thermal evaporation process. Electrical characterisation and surface morphology verifications were then carried out on the samples by Hall effect measurement and atomic force microscopy (AFM). It was found that the conductivity of the Al-doped Si increases with increasing Al/Si ratio and the resulting hole concentration ranges from 10^{18} up to 10^{21} atoms/cm^3. AFM data shows root mean square (RMS) surface roughness of 9-13 nm, independent of Al/Si ratio. The roughness observed shows surface characteristics produced by the thermal evaporation technique. The effects of the observed properties towards the fabrication of base layer (p-type) in thin film Si solar cells on PET were subsequently discussed.

1. Introduction

Doping is a process of intentionally introducing impurities into a pure semiconductor (intrinsic) in order to alter its electrical properties. Doping process can be introduced from various sources; solid source dopants, spin-on chemical dopants, ion implantation and also by metal-doping process. To make a p-type silicon (Si), conventional boron diffusion doping (either by solid source or spin-on chemical) normally demands a long processing time with high temperature requirement (>950°C). This process is very costly and can be detrimental to Si too [1]. Ion implantation is a complicated process and also expensive. Metal-doping is normally in favor for a process involving low-temperature limiting substrates such as polyethylene terephthalate (PET). A low melting point of 250-260°C [2] of PET places temperature constraints to the overall process flow that uses it as a substrate. This makes the metal-doping approach as a more appealing option to realize the doping of the film on PET.

Metal-doping is oftenly realised by two ways. The first way is called metal-induced crystallization (MIC) technique; involves evaporating a thin metal layer upon a layer of Si which has been previously deposited onto a particular substrate. These two layers are then annealed at a very low temperature for some duration, finally produces a metal-doped Si layer (e.g. Al-doped Si) [3]. The second way is by direct alloying metal-semiconductor in a single process step (e.g. co-evaporation, co-sputtering) where both elements are mixed and deposited under controlled composition to produce the intended level of carrier concentration [4].

The aim of this work is to study the feasibility of producing a p-type thin film Si layer on PET via a simple thermal evaporation process and to analyse the electrical properties (i.e. hole concentration and hole mobility) and surface morphologies of the films with different Al doping levels. The optimised Al-doped Si process parameters will later be used in the fabrication of base layer of thin film Si solar cells on PET. Feasibility of this technique on such a low-cost substrate will help to expedite the cost reduction of Si photovoltaics technology further towards grid parity. Related works with the same objective of cost reduction (due to elimination of sophisticated chemical vapor deposition technique, CVD, for Si absorber layer fabrication) are still being heavily researched in the ARC Photovoltaics Centre of Excellence at UNSW (Sydney) laboratory by using electron beam (E-Beam) evaporation technique [5,6,7].

2. Experimental methods

In this experiment, PET of 250 μm thickness from Penfibre Sdn. Bhd. (Film Division) was used as a substrate for the p-type thin film Si fabrication. The PET substrates were firstly cleaned by being fully immersed in Decon 90 for 10 minutes to remove contamination. After the cleaning process, all the substrates were rinsed with deionized water (DIW) to remove the residue of Decon 90. The samples were then dipped in isopropyl alcohol (IPA) and agitated with medium ultrasonic power for 10 minutes. The samples were again dipped in DIW and then dried off with nitrogen (N$_2$) gas after the ultrasonic cleaning.

Si powder (325 mesh with 99% trace metal basis from Sigma Aldrich) and Al rods (99.9% purity,

M=26.98g/mol) were prepared for thermal evaporation process. Before mixing the Al and Si powder, the Al rods were cut into very small pieces (as small as possible). The purpose was to ensure an even mixture of Al and Si powder in the tungsten boat for the evaporation process. This step is very crucial since an even mixture of both elements will help to produce a film with uniform doping on the PET substrate.

```
        ┌─────────────────────────┐
        │   Al-doped thin film Si  │
    ┌───┴─────────────────────────┴───┐
    │              PET                 │
    └──────────────────────────────────┘
```
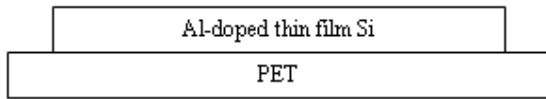
Fig. 1. Basic representation of Al-doped thin film Si thermally evaporated on PET substrate (Figure not drawn to scale).

In this experiment, 5 samples of different Al doping levels were prepared with Al/Si ratio of 0.05, 0.1, 0.2, 0.3 and 0.4. The Al/Si ratio was controlled by controlling the weight of Al over the weight of Si powder with the weight of Si kept fixed for all the samples. The mixtures were then thermally evaporated by Edward Auto 306 thermal evaporation system at the base pressure of 1.5×10^{-5} Torr as represented by Fig. 1 above. Al contacts were then evaporated on every sample for Hall effect measurement. The contact evaporation process was also carried out on the same system at the base pressure of 2.7×10^{-5} Torr.

After contact evaporation process, the samples were annealed in N_2 ambient at 200 ^{o}C for 2 hours on Lenton VTF annealing tube furnace to ensure good contact properties and good film adhesion on PET. Besides, annealing in this condition helps to improve the distribution of Al atoms in the Si lattice after the evaporation process thus ensures a better doping uniformity across the substrate. Thickness measurements were carried out on all the samples by using Filmetrics F20 optical reflectometer. The thin films were then electrically characterised on Accent HL 5500 PC Hall effect measurement system to measure the values of resistivity, carrier concentration and carrier mobility. The surface morphologies of the films were viewed and analyzed under ULTRA Objective atomic force microscope (AFM) system.

3. Results and discussion

Thickness of the films produced by the thermal evaporation processes were measured to be in the range of 4-5 μm respectively. Table 1 below summarises the electrical properties of the films and the following Fig. 2 and Fig. 3 are plotted to graphically illustrate the results in Table 1.

Table 1. Electrical properties of thermally evaporated Al-doped thin film Si on PET.

Sample	Al/Si ratio	Resistivity (x 10^{-3} Ω.cm)	Sheet mobility (cm^2/Vs)	Carrier concentrations (atoms/cm^3)	Remarks
Sample 1	0.05	~MΩ.cm	cannot be measured	cannot be measured	Insulator
Sample 2	0.10	14.43	46.10	5.76×10^{18}	Heavily-doped p+-type semiconductive film
Sample 3	0.20	8.28	33.80	1.26×10^{19}	Heavily-doped p+-type semiconductive film
Sample 4	0.30	1.07	14.60	7.62×10^{20}	Heavily-doped p++-type semiconductive film
Sample 5	0.40	0.62	9.54	3.24×10^{21}	Heavily-doped p++-type semiconductive film

From the table, it can be observed that the resulting film's resistivity reduces from 14.43×10^{-3} to 0.62×10^{-3} Ω.cm as the Al/Si ratio increases from 0.1 to 0.4. The film with Al/Si ratio 0.05 appears to be an insulator with resistivity in the 10^6 range. This could be due to insufficient amount of Al dopant atoms in the sample to produce a conductive film. Apart from that, the presence of grain boundaries and other embedded intrinsic defects may increase the resistivity of the film as commonly encountered at low doping level in Si lattice [8].
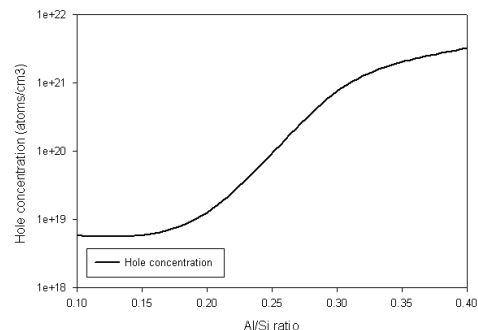
Fig. 2. Hole concentration of the Al-doped thin film Si on PET at different Al/Si ratios.
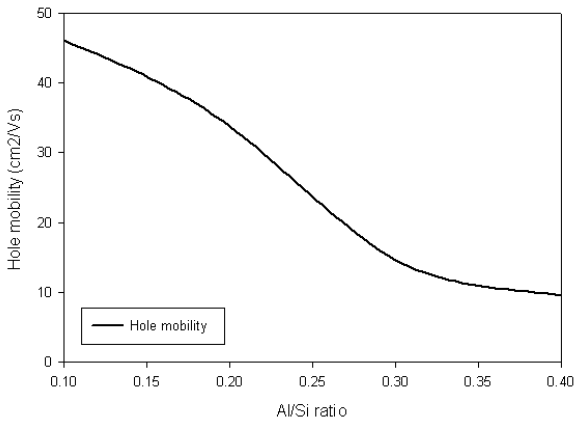
Fig. 3. Hole mobility of the Al-doped thin film Si on PET at different Al/Si ratios.

Fig. 4. AFM images (5 × 5 μm spot size) of the Al-doped thin film Si on PET at different Al/Si ratios.

Fig. 2 illustrates that with increasing Al/Si ratio from 0.1 to 0.4, the hole concentration also increases from as low as 5.76×10^{18} up to 3.24×10^{21} atoms/cm^3. The minimum hole concentration in order of 10^{18} atoms/cm^3 obtained in this result is quite high for the fabrication of p-type base in thin film Si solar cells where the hole concentration normally lies in the range of 10^{15}-10^{17} atoms/cm^3 [9]. The base with higher doping concentration introduces more undesirable trap states which promotes more recombination processes hence reduces the carrier diffusion lengths and lifetimes [10]. Low carrier diffusion lengths and lifetimes are normally observed in Al-doped Si wafers due to the generation of a recombination-active defect complex made up of Al and oxygen (O) during the doping process [11]. The generation of trap states and defect-complex are detrimental to the solar cells since they will cause sharp reduction in the value short-circuit current (I_{sc}) thus reducing the conversion efficiency of the cells.

From Fig. 3, it can be seen that the value of hole mobility reduces from 46.1 to 9.54 cm^2/Vs as the hole concentration increases in the films as expected. The reducing hole mobility with increasing hole concentration observed corroborates quite well with the data published by Dorkel et al. [12]. The reduction in hole mobility is due to the fact that at high doping level, band tails are introduced in the form of density of states within the band gap near both band edges due to the random distribution of dopant ions. Hence, minority carriers from photogeneration process tend to be confined within this region, where the states have a localized character [13]. This observation can also be explained by band gap-narrowing and intense carrier-to-carrier interactions at high doping level [14]. Thus, a reduction in mobility is expected.
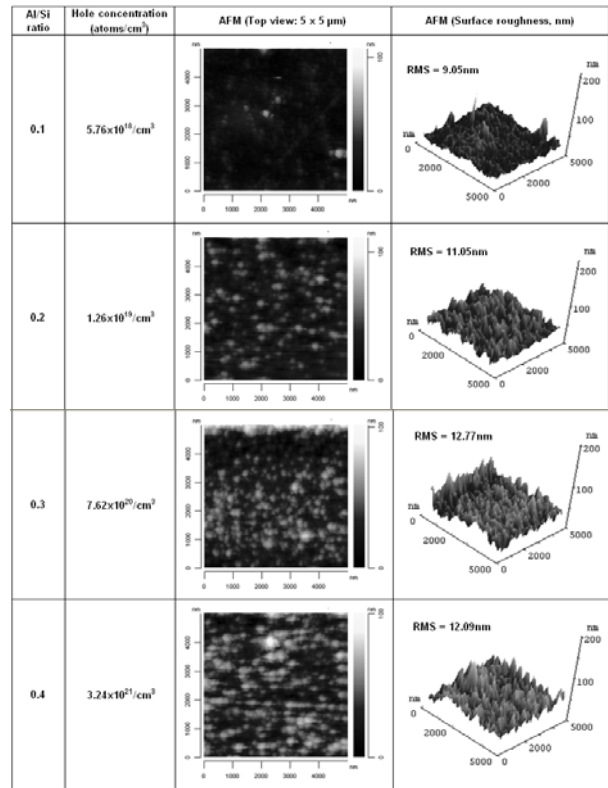
Fig. 4 shows the surface morphologies of the thin films on PET at different Al/Si ratios viewed under AFM with the spot size of 5 × 5 um. All the samples show self-roughened and textured surfaces with RMS surface roughness of 9-13 nm, independent of Al/Si ratio being used. Lateral feature size of the samples were observed to range from 200-500 nm, normally can be increased further to micron level by higher temperature or prolonged annealing treatment. Typical RMS values of textured surfaces in thin film Si solar cells reported in the literature are in the range of 50-90 nm with lateral feature sizes of 300-500 nm for amorphous Si and 1000-1400 nm for micromorph-type solar cells [15]. High surface roughness is highly desirable in the fabrication of thin film Si solar cells because rougher surface enhances light-trapping properties of the film by multiple-fold (i.e. higher optical path length), reduces reflection losses of the solar cell. Improved light-trapping increases potential for the impinging photons to be harvested; i.e. to excite valence electrons to conduction band and yields the intended photocurrent [16]. On the other hand, higher lateral feature size reflects higher grain size (or lower number of grain boundaries) within the film. This corresponds to lower availability of recombination centres that will reduce the resulting output current significantly.

The AFM images also show increasing brightness with increasing Al/Si ratio. The increase in the image brightness results from the increase in the number of Al

dopant atoms (crystallites) distributed within the Si thin film. This observation suggests that surface reflection from the Al crystallites in the films should increase correspondingly since the Al atom (or Al film) is an effective light reflector or mirror [17,18]. Therefore, the surface reflection properties at various Al/Si ratios have to be studied further so that the optimum amount of Al dopant atoms (in Al/Si ratio) can be used to get the intended p-type (base layer) doping level and at the same time does not produce an intolerable reflection that will subsequently reduce the photocurrent generation within the film.

4. Conclusions

In this experiment, Al-doped Si (p-type) thin films of various doping levels have been successfully prepared by thermal evaporation technique. Results show that the conductivity of the Al-doped Si increases with increasing Al/Si ratio and the corresponding hole concentration of 10^{18} to 10^{21} atoms/cm^3 are produced. However, 10^{18} atoms/cm^3 can be considered quite high and not very suitable as the base layer (p-type) of thin film Si solar cells since it will generate more trap states thus induces more recombination activities inside the film. AFM data of all the samples show low RMS surface roughness of about 9-13 nm with low lateral feature size, independent of Al/Si ratio. Even though all the films show self-roughened properties, this analysis alone will not be adequate without surface reflection data. Low reflection losses are desirable in solar cells in order to maximise the generation of output current from the cell.

References

[1] James M. Gee, Michel D. Bode, Beverly L. Silva, 26th IEEE Photovoltaic Specialists Conference, 1-4 (1997).
[2] Ruey-Shi Tsai, Da-Kong Lee, Han-Yu Fang, Hong-Bing Tsai, Asia-Pac. J. Chem. Eng. **4**, 140 (2008).
[3] Hameed A. Naseem, M. Shahidul Haque, William D. Brown, United States Patent US6,613,653 B2, (2003).
[4] F. Lin, M. K. Hatalis, S. Girginoudi, D. Girginoudi, N. Georgoulas, A. Thanailakis, Mat. Res. Soc. Symp. Proc. **230**, (1992).
[5] O. Kunz, Z. Ouyang, J. Wong, A. Aberle, Advances in Optoelectronics, 532351 (2008).
[6] A. G. Aberle, Thin Solid Films **26**, 511 (2006).
[7] P. I. Widenborg, A. G. Aberle, Journal of Crystal Growth **242**, 270 (2002).
[8] Jenny Nelson, The Physics of Solar Cells, Imperial College Press, (2003).
[9] M. Birkholz, B. Selle, W. Fuhs, S. Christiansen, H. P. Strunk, R. Reich, Physical Review B **64**, (2006).
[10] C. H. Henry, D. V. Lang, Physical Review B **15**, 989 (1977).
[11] J. R. Davis, IEEE Trans. Electron Devices ED **27**, 677 (1980).
[12] J. M. Dorkel, Ph. Leturcq, Solid State Electron **24**, 821 (1981).
[13] A. Neugroschel, F. A. Lindholm, Appl. Phys. Lett. **42**, 176 (1983).
[14] J. Van Meerbergen, J. Nijs, R. Mertens, R. Van Overstraeten, 13th IEEE Photovoltaic Specialists Conference, 66 (1978).
[15] Vanessa Terrazzoni-Daudrix, Joelle Guillet, Xavier Niquille, Arvind Shah, Mat. Res. Soc. Symp. Proc. **769**, (2003).
[16] E. Yablonovitch, J. Opt. Soc. Am. **72**, 899 (1982).
[17] Z. Ouyang, O. Kunz, M. Wolf, J. Guangyao, P. Widenborg, S. Varlamov, Proc. 18th International Photovoltaic Science and Engineering Conference (PVSEC), (2009).
[18] R. M. Swanson, R. A. Sinton, Advances in Solar Energy **6**, 427 (1990).

_____

*Corresponding author: zamirlitho@gmail.com